A&A, 710, L5 (2026)
https://doi.org/10.1051/0004-6361/202660036

Astronomy & Astrophysics

LETTER TO THE EDITOR

The magnetic fields in Be stars are stronger than previously suggested

S. Hubrig[1,⋆], S. P. Järvinen[1], M. Schöller[2], and I. Ilyin[1]

[1] Leibniz-Institut für Astrophysik Potsdam (AIP), An der Sternwarte 16, 14482 Potsdam, Germany
[2] European Southern Observatory, Karl-Schwarzschild-Str. 2, 85748 Garching, Germany

Received 24 March 2026 / Accepted 24 April 2026

ABSTRACT

Context. Recent observational studies suggest that Be stars most likely are formed through the process of mass transfer in binary systems. In view of the wide consensus that the origin of the magnetic field in stars with radiative envelopes involves binary interaction processes, searching for magnetic fields in Be stars appears especially promising.
Aims. As a pilot project, we searched for the presence of magnetic fields in a sample of seven well-known Be stars.
Methods. We used high-resolution HARPSpol spectra to measure the mean longitudinal magnetic field, employing the least squares deconvolution technique. A dedicated measurement procedure introduced by our group in recent years was applied.
Results. Opposite to previous spectropolarimetric studies reporting that magnetic fields in Be stars are weak and usually below 100 G, our study presents the first observational evidence that magnetic fields in Be stars can be as strong as a few hundred gauss. Magnetic fields are detected in all studied Be stars, with the strongest magnetic field being about −460 G for the B0.5 III star HD 184915. Magnetic fields in the range between 338 and 380 G (in absolute values) are detected in three other Be stars, HD 209409, HD 209522, and HD 224686. Due to the fact that magnetic fields in Be stars are stronger than previously believed, we must re-evaluate our understanding of the initial conditions of massive binaries to be able to determine the origin of such systems.

Key words. techniques: polarimetric – binaries: general – stars: early-type – stars: emission-line, Be – stars: magnetic field – starspots

1. Introduction

Be stars are defined as rapidly rotating main sequence stars showing normal B-type spectra with superposed Balmer line emission. These stars are furthermore characterized by the episodic dissipation and formation of a circumstellar disk-like environment called the Keplerian decretion disk, non-radial pulsations (NRPs), and photometric and spectroscopic variability. Several scenarios have been suggested to explain the accumulation of material in equatorial disks around Be stars. Cassinelli et al. (2002) suggested a magnetically torqued disk model, in which a sufficiently strong magnetic field (of the order of 300 G) channels a flow of wind material towards the equatorial plane to form a disk. The study of a variety of stellar models by Maheswaran & Cassinelli (2009) showed that in the disk region that is initially formed when wind material is channeled by dipole-type magnetic fields towards the equatorial plane, magnetorotational instability can set in and assist in the formation of a quasi-steady disk. Magnetic fields as weak as a few tens of gauss will be able to channel wind flow into a proto-disk region. Another scenario involves NRPs, which seem to be a key aspect of the mass ejection mechanism (e.g. Labadie-Bartz et al. 2022; Saio 2024). On the other hand, numerous, more recent studies indicate that Be stars most likely form through mass transfer in binary systems, and many of them are now seen as parts of binary systems comprising a lower-mass stripped-envelope companion star (e.g. Labadie-Bartz et al. 2025). In this case, it is possible that the rapid rotation of Be stars is related to the binarity interaction and that their decretion disk is formed due to the impact of accretion. Yet, according to Xing et al. (2026), mass transfer between two non-degenerate stars is an insufficiently understood process within the framework of binary evolution, and a detailed description of the accretion process would require dedicated multi-dimensional hydrodynamical simulations.

Observational evidence that a significant fraction of Be stars are products of binary mass transfer is especially intriguing in view of the wide consensus that the origin of the magnetic field in stars with radiative envelopes involves mass transfer, a common envelope evolution, or a merging event (e.g. Tout et al. 2008; Ferrario et al. 2009; Schneider et al. 2016). On the observational side, Hubrig et al. (2023, 2026) analyzed representative samples of O- and B-type systems at different stages of interaction using the HARPSpol spectrograph attached to the ESO 3.6 m telescope (Snik et al. 2008) and, based on the numerous magnetic field detections, concluded that interaction between the system components plays a definite role in the generation of magnetic fields in massive O and B stars. Previous analyses of low-resolution spectropolarimetric data of Be stars obtained with the ESO multi-mode instrument FORS1 by Hubrig et al. (2007, 2009) revealed the presence of weak magnetic fields in seven Be stars: HD 62367, μ Cen, o Aqr, ϵ Tuc, 27 CMa, χ Oph, and V 1075 Sco. These studies suggested that the magnetic fields of Be stars are not strong, usually below 100 G. The strongest longitudinal magnetic field, $\langle B_z \rangle = 146 \pm 32$ G, was detected in the Be star 27 CMa. Later on, Wade et al. (2016) analyzed high-resolution spectropolarimetric data for 85 Be stars

⋆ Corresponding author: shubrig@aip.de

using the multi-line least-squares deconvolution (LSD) method (Donati et al. 1997) and found no evidence of a magnetic field in any of the studied stars. Notably, Wade et al. (2016) used masks with photospheric lines belonging to different elements altogether, while the more recent analyses by Hubrig et al. (2023, 2026) followed a dedicated procedure involving for each target different line masks populated for each element separately.

To test the influence of interaction processes on the generation of magnetic fields in massive stars, we initiated as a pilot project a spectropolarimetric study of a sample of seven well-known Be stars. The paper is laid out as follows: We present our HARPSpol spectropolarimetric observations, their reduction, and the magnetic field measurements for each individual target in Sect. 2. The results of the measurements of the studied Be stars, the distribution of their magnetic field strengths, and the implication of the field detections for the origin of Be stars are briefly discussed in Sect. 3.

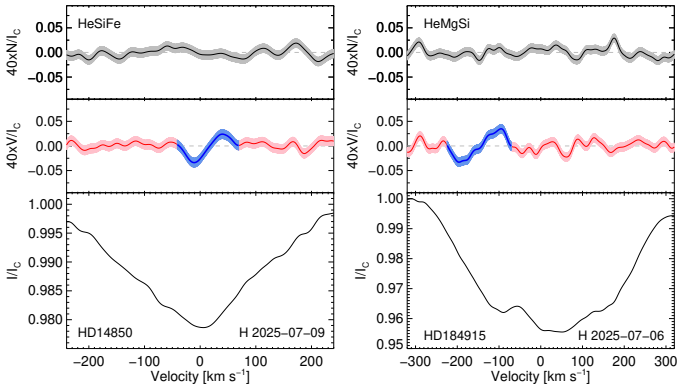

Fig. 1. Results of the LSD analysis for the Be stars HD 14850 (left) and HD 184915 (right). Stokes I, Stokes V, and diagnostic null N spectra were obtained for the line masks indicated in the plots. The identified Zeeman signatures are in blue.

2. Observations and magnetic field measurements

We used HARPSpol from July 6 to July 9 in 2025 to obtain circular polarized spectra of seven Be stars. HARPSpol has a resolving power of about 115 000 and a wavelength coverage from 3780 to 6910 Å with a small gap between 5259 and 5337 Å. With these data, we have access to measurements of the mean longitudinal magnetic field, $\langle B_z \rangle$, which is the line-of-sight component of the magnetic field weighted with the line intensity and averaged over the visible hemisphere. Additionally, we retrieved from the Canada-France-Hawaii Telescope (CFHT) science archive ESPaDOnS (the Echelle SpectroPolarimetric Device for Observations of Stars) observations of HD 205637 from 2011 covering the wavelength range from 3750 to 10 500 Å with a spectral resolution of about 65 000. As in our previous studies that used HARPSpol data (e.g. Hubrig et al. 2018; Järvinen et al. 2018), we employed the LSD technique following the description given by Donati et al. (1997) in order to increase the accuracy of the mean longitudinal magnetic field determination. The parameters of the lines used to calculate the LSD profiles were taken from the Vienna Atomic Line Database (VALD3; Kupka et al. 2011). All of our targets show the presence of a proper motion anomaly (Kervella et al. 2019), indicating probable membership in binary systems, as expected for Be stars. Thus, we applied for the treatment of their spectra a dedicated procedure similar to that described by Hubrig et al. (2023, 2026). Its measurements involve different line masks populated for each element separately. Such a strategy is also frequently employed in the studies of B-type stars hosting magnetic fields, where abundance anomalies are associated with the presence of surface chemical patches. The distribution of such patches is non-symmetric with respect to the rotation axis but shows a correlation with the magnetic field topology (e.g. Rice et al. 1997; Hubrig et al. 2012, 2017). As the visibility of the patches is changing during the stellar rotation, different line masks should be tested. More details about our LSD analysis are presented in Appendix A.

The presence of a magnetic field in the LSD profile was evaluated according to Donati et al. (1992), who defined a Zeeman profile with a false alarm probability (FAP) of $\leq 10^{-5}$ as a definite detection, whereas $10^{-5} < \mathrm{FAP} \leq 10^{-3}$ is a marginal detection, and $\mathrm{FAP} > 10^{-3}$ is a non-detection. A summary of our measurements is presented in Table 1. In the following, we discuss for each target the spectral appearance, previously known properties, and the results of the measurements.

HD 14850 (= CPD–30 286): The spectrum of this B8 IIIe high Galactic latitude star (Slettebak et al. 1997), shown in Fig. B.1, exhibits strong emission in the Hα line and emission in the Fe II lines at 6456 and 6516 Å, which are frequently identified in the spectra of Be stars. We achieved for this star a definite magnetic field detection with $\langle B_z \rangle = -59 \pm 84$ G using a mask containing He, Si, and Fe lines. Our LSD analysis is presented in Table 1 and the left panel of Fig. 1.

HD 184915 (= κ Aql): As we show in Fig. B.2, we detect in our HARPSpol spectrum of this target weak emission on both sides of the Hα line and in the blue wings of the Si III triplet lines. Notably, numerous lines show a distinct structure, which can probably be explained by the presence of a companion or the presence of NRPs similar to pulsations observed in β Cep and slowly pulsating B stars. The presence of NRPs is frequently determined through observations of moving peaks in the cores of spectral lines. From the theoretical considerations presented by Hubrig et al. (2004), it follows that pulsationally modulated variations of the order of 100 G may exist in the outer atmospheric layers of stars with kilogauss-scale magnetic fields. On the observational side, Shultz et al. (2017) studied the impact of pulsations for the β Cephei pulsator HD 46328 and showed that at some observing epochs the measured longitudinal magnetic field can vary by about ±2–3%.

According to de Burgos et al. (2024), this target is enriched in helium, suggesting that it might be a product of binary evolution. Of all the targets studied, HD 184915 possesses the strongest longitudinal magnetic field, $\langle B_z \rangle = -461 \pm 59$ G. The field was definitely detected using a mask containing He, Mg, and Si lines. Our LSD analysis is presented in Table 1 and the right panel of Fig. 1.

HD 205637 (= ϵ Cap): The presence of a companion with an orbital period of 128.5 d was previously reported in Rivinius et al. (2006). Our spectra also show a change in the radial velocity between 2011 and 2025. Apart from the HARPSpol observation, this target was also observed on one night in June 2011 with ESPaDOnS. It was recorded five times using consecutive short exposures with 10 min durations. Figure B.3 shows that the emission in the Hα and He I 6678 line profiles were stronger in 2011 than in 2025. It is of interest that Buscombe (1969) classified this target as a shell star with sharp

Table 1. Observations and results of the magnetic field measurements for all targets in our sample.

HD number	Spectral type	m_V	MJD	Instr.	S/N	Line mask	FAP	Det. flag	$\langle B_z \rangle$ [G]
14850	B8IIIe	8.40	60865.418209	H	162	HeSiFe	9×10^{-7}	DD	-59 ± 84
184915	B0.5IIIn	4.97	60862.387233	H	245	HeMgSi	1×10^{-6}	DD	-461 ± 59
205637	B3V	4.55	55723.535672	E	481	HeSiFe	$<10^{-10}$	DD	-85 ± 11
			60863.387768	H	422	HeMgFe	7×10^{-7}	DD	-28 ± 7
209014	B8IIIsh+B8.5IV	5.42	60863.438702	H	477	MgSiFe	7×10^{-6}	DD	38 ± 87
209409	B5V	4.69	60863.371608	H	413	HeMgSiCrFe	6×10^{-6}	DD	338 ± 49
209522	B4IVe	5.95	60865.373670	H	332	HeCSiFe	2×10^{-6}	DD	-380 ± 71
224686	B8V	4.47	60863.406779	H	482	SiFe	6×10^{-9}	DD	375 ± 109

Notes. Column 1: HD number of the star. Column 2: Spectral type taken from SIMBAD. Column 3: Visual magnitude. Column 4: MJD values at the middle of the exposure. Column 5: Instrument used, where H stands for HARPSpol and E for ESPaDOnS. Column 6: Signal-to-noise ratio measured in the Stokes I spectra in the spectral region around 5000 Å. Column 7: Applied line masks. Column 8: FAP values. Column 9: Detection flag, where DD means a definite detection. Column 10: Measured LSD mean longitudinal magnetic field strength.

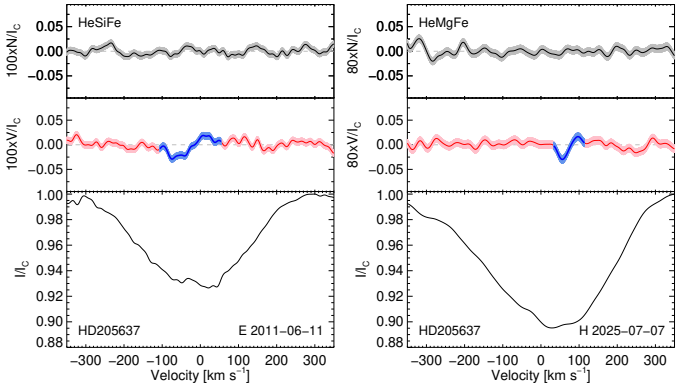

Fig. 2. LSD analysis of HD 205637 using ESPaDOnS (left) and HARPSpol (right) observations.

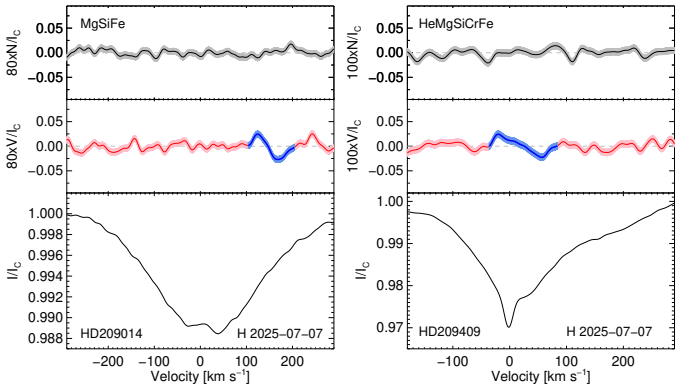

Fig. 3. Same as Fig. 1 but for HD 209014 (left) and HD 209409 (right).

absorption lines formed in the surrounding gaseous shell. It has been suggested that the appearance of a Be star as a shell star can be determined from the inclination angle of the disk (e.g. Hanuschik 1995). No changes between the five ESPaDOnS spectra acquired over 0.8 h have been detected. We achieved for HD 205637 definite detections with $\langle B_z \rangle = -85 \pm 11$ G using the ESPaDOnS observations with a He, Si, and Fe mask and $\langle B_z \rangle = -28 \pm 7$ G using the HARPSpol observations and a mask containing He, Mg, and Fe lines. The results of our analysis are presented in Table 1 and Fig. 2.

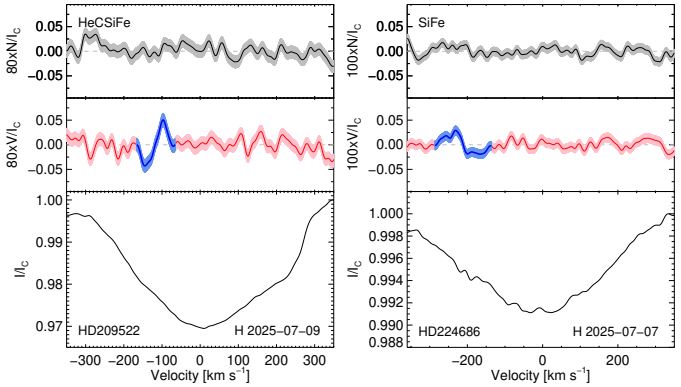

Fig. 4. Same as Fig. 1 but for HD 209522 (left) and HD 224686 (right).

HD 209014 (= η PsA): According to Corbally (1984), this target is a close visual binary system with a primary B8 IIIsh star and a B8.5 IV companion. As we show in Fig. B.4, the Hα line in the HARPSpol spectrum is in emission and the profile of the Fe II 5018 line displays emission in both the red and blue wings. We achieved for this target a definite magnetic field detection with $\langle B_z \rangle = 38 \pm 87$ G using a mask containing Mg, Si, and Fe lines. The results of our analysis are presented in Table 1 and the left panel of Fig. 3.

HD 209409 (= o Aqr): Cowley et al. (2015) consider this bright target to be a prototype Be shell star. While Hα is in emission and the Fe II 5018 profile in Fig. B.5 shows a typical sharp shell core together with emission wings, other Balmer lines exhibit sharp absorption cores, much sharper than expected from the widths of normal photospheric lines. The He I lines are broad and shallow, unlike the metal lines, indicating an atmospheric origin. The Stokes I profile in Fig. 3 shows a composite line profile structure. Using low-resolution spectropolarimetric observations with FORS1, Hubrig et al. (2009) detected a weak magnetic field, $\langle B_z \rangle = -98 \pm 31$ G. Our analysis of high-resolution HARPSpol observations confirms the magnetic nature of HD 209409 thanks to our definite magnetic field detection with $\langle B_z \rangle = 338 \pm 49$ G using a mask containing He, Mg, Si, Cr, and Fe lines. The results of our analysis are presented in Table 1 and the right panel of Fig. 3.

HD 209522 (= UU PsA): According to Shokry et al. (2018), who studied the stellar parameters of Be stars observed with X-shooter, no recent study has found Balmer emission in this star. However, Hα emission is clearly detected in our HARPSpol spectrum (see Fig. B.6). We also observe a weak emission in the red wing of the Fe II line at 5018 Å. We achieved for this star a definite magnetic field detection with $\langle B_z \rangle = -380 \pm 71$ G using a mask containing He, C, Si, and Fe lines. The results of our analysis are presented in Table 1 and the left panel of Fig. 4.

HD 224686 (= ϵ Tuc): As shown in Fig. B.7, the HARPSpol spectrum of this target displays characteristics of shell stars, with the Hα line exhibiting sharp absorption cores, much sharper than expected from the width of normal photospheric lines. Furthermore, Fe II lines belonging to Multiplet 42 show the presence of central emission. While Buscombe (1969) classified this target as B7Vke with a note that Hα is in emission, almost a decade later, Pedersen (1978) presented an Hα line profile similar to that detected in our observations. The detection of a weak longitudinal magnetic field in HD 224686 with $\langle B_z \rangle = 74 \pm 24$ G was previously reported by Hubrig et al. (2009). We achieved for this star a definite magnetic field detection with $\langle B_z \rangle = 375 \pm 109$ G using a mask containing Si and Fe lines. The results of our analysis are presented in Table 1 and the right panel of Fig. 4.

3. Discussion

In this work, we present observational evidence that Be stars can possess magnetic fields of the order of a few hundred gauss. We also confirm the presence of a magnetic field in two targets, HD 209409 and HD 224686, previously observed with FORS1. Magnetic fields in five Be stars have been measured for the first time. HD 184915 has the strongest magnetic field, of about −460 G, followed by HD 209409, HD 209522, and HD 224686 with field strengths above 300 G in absolute values. Apart from HD 205637, our targets have been observed only once. Since, per definition, the longitudinal magnetic field is strongly dependent on the viewing angle between the field orientation and the observer and is modulated as the star rotates, its magnetic field could be even stronger.

In all LSD plots, the detected Zeeman signatures do not extend over the full LSD Stokes I profile. As mentioned in Sect. 2, this is explained by the fact that magnetic A- and B-type stars usually show a rotationally modulated appearance of chemical patches. On the other hand, since all targets in our sample are reported to show a proper motion anomaly, the shifted locations of the observed Zeeman signatures relative to the underlying Stokes I profiles probably indicate that some of our targets are close binaries with magnetic components.

Four targets in our sample, HD 205637, HD 209014, HD 209409, and HD 224686, currently display or displayed characteristics of shell stars. Importantly, magnetic fields have previously been detected in two other shell Be stars, the visual binary 27 CMa with $\langle B_z \rangle = -146 \pm 32$ G using FORS1 spectropolarimetry (Hubrig et al. 2007) and in HD 61954 using HARPSpol observations with $\langle B_z \rangle = 156 \pm 46$ G and $\langle B_z \rangle = -420 \pm 95$ G measured on two different nights (Hubrig et al. 2025). HD 61954 is, however, a well-known blue straggler star in the open cluster NGC 2437, for which mass transfer from a binary companion has probably led to the rejuvenation of the mass gainer. Based on the reported magnetic field detections in targets with shell spectra, it is possible that other Be stars with shell-like line profiles are also products of interaction and therefore possess magnetic fields.

The origin of fast-rotating Be stars with decretion disks remains unclear. According to Labadie-Bartz et al. (2025), there are two classes of Be binaries, pre-interaction and post-interaction. Given the detection of magnetic fields in Be stars, a crucial improvement of our understanding of the initial conditions of massive binaries is required to be able to determine the origin of such systems.

Acknowledgements. This work is based on observations made with ESO telescopes at the La Silla Paranal Observatory under programme ID 0115.D-2108(A). Observations of HD 205637 were also obtained with CFHT, which is operated by the National Research Council of Canada, the Institut National des Sciences de l'Univers of the Centre National de la Recherche Scientifique of France, and the University of Hawaii.

References

Buscombe, W. 1969, MNRAS, 144, 1
Cassinelli, J. P., Brown, J. C., Maheswaran, M., Miller, N. A., & Telfer, D. C. 2002, ApJ, 578, 951
Corbally, C. J. 1984, ApJS, 55, 657
Cowley, C. R., Przybilla, N., & Hubrig, S. 2015, A&A, 578, A26
de Burgos, A., Simón-Díaz, S., Urbaneja, M. A., & Puls, J. 2024, A&A, 687, A228
Donati, J. F., Semel, M., & Rees, D. E. 1992, A&A, 265, 669
Donati, J. F., Semel, M., Carter, B. D., Rees, D. E., & Collier Cameron, A. 1997, MNRAS, 291, 658
Ferrario, L., Pringle, J. E., Tout, C. A., & Wickramasinghe, D. T. 2009, MNRAS, 400, L71
Hanuschik, R. W. 1995, A&A, 295, 423
Hubrig, S., Kurtz, D. W., Bagnulo, S., et al. 2004, A&A, 415, 661
Hubrig, S., Yudin, R. V., Pogodin, M., Schöller, M., & Peters, G. J. 2007, Astron. Nachr., 328, 1133
Hubrig, S., Schöller, M., Savanov, I., et al. 2009, Astron. Nachr., 330, 708
Hubrig, S., González, J. F., Ilyin, I., et al. 2012, A&A, 547, A90
Hubrig, S., Przybilla, N., Korhonen, H., et al. 2017, MNRAS, 471, 1543
Hubrig, S., Järvinen, S. P., Madej, J., et al. 2018, MNRAS, 477, 3791
Hubrig, S., Järvinen, S. P., Ilyin, I., Schöller, M., & Jayaraman, R. 2023, MNRAS, 521, 6228
Hubrig, S., Järvinen, S. P., Ilyin, I., & Schöller, M. 2025, A&A, 701, A255
Hubrig, S., Abdul-Masih, M., Järvinen, S. P., et al. 2026, A&A, 707, A3
Järvinen, S. P., Hubrig, S., Ilyin, I., et al. 2018, A&A, 618, L2
Kervella, P., Arenou, F., Mignard, F., & Thévenin, F. 2019, A&A, 623, A72
Kupka, F., Dubernet, M. L., & VAMDC Collaboration 2011, Balt. Astron., 20, 503
Labadie-Bartz, J., Carciofi, A. C., Henrique de Amorim, T., et al. 2022, AJ, 163, 226
Labadie-Bartz, J., Suffak, M., Jones, C., et al. 2025, Ap&SS, 370, 134
Maheswaran, M., & Cassinelli, J. P. 2009, MNRAS, 394, 415
Pedersen, H. 1978, A&A, 63, 305
Rice, J. B., Wehlau, W. H., & Holmgren, D. E. 1997, A&A, 326, 988
Rivinius, T., Štefl, S., & Baade, D. 2006, A&A, 459, 137
Saio, H. 2024, https://doi.org/10.5281/zenodo.13853246
Schneider, F. R. N., Podsiadlowski, P., Langer, N., Castro, N., & Fossati, L. 2016, MNRAS, 457, 2355
Shokry, A., Rivinius, T., Mehner, A., et al. 2018, A&A, 609, A108
Shultz, M., Wade, G. A., Rivinius, T., et al. 2017, MNRAS, 471, 2286
Shultz, M. E., Wade, G. A., Rivinius, T., et al. 2018, MNRAS, 475, 5144
Slettebak, A., Wagner, R. M., & Bertram, R. 1997, PASP, 109, 1
Snik, F., Jeffers, S., Keller, C., et al. 2008, SPIE Conf. Ser., 7014, 70140O
Tout, C. A., Wickramasinghe, D. T., Liebert, J., Ferrario, L., & Pringle, J. E. 2008, MNRAS, 387, 897
Wade, G. A., Petit, V., Grunhut, J. H., Neiner, C., & MiMeS Collaboration 2016, ASP Conf. Ser., 506, 207
Xing, Z., Fragos, T., Kalogera, V., et al. 2026, arXiv e-prints [arXiv:2602.06259]

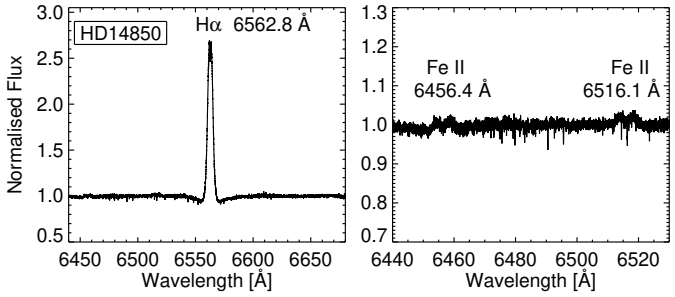

Fig. B.1. HARPSpol Stokes *I* spectrum of the B8 IIIe star HD 14850, which exhibits emission in the Hα line and the Fe II lines at 6456 and 6516 Å. These emission lines are frequently identified in the spectra of Be stars.

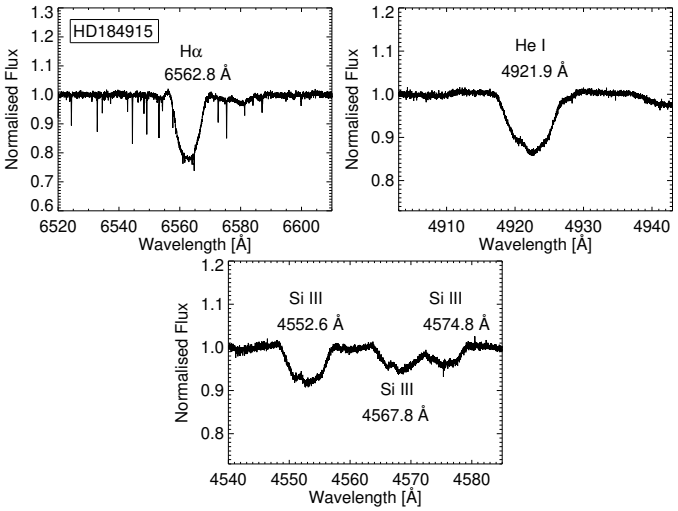

Fig. B.2. HARPSpol Stokes *I* spectrum of the B0.5 IIIn star HD 184915, which shows the presence of weak emission on both sides of the Hα line and in the blue wings of the Si III triplet lines.

Appendix A: Selection of spectral lines to populate line masks

Significant differences in the magnetic field strengths measured in B-type stars using spectral lines belonging to different elements were previously mentioned in numerous studies (e.g. Hubrig et al. 2017; Shultz et al. 2018). As shown by these authors, magnetic field phase curves obtained using spectral lines of individual elements can even show variability in antiphase. This is possible if chemical abundance patches with a concentration of individual elements have a different distribution in horizontal or vertical direction, depending on the magnetic field configuration and the atmospheric structure of the star. Taking into account that lines belonging to different elements can show dispersion in the measured longitudinal magnetic fields, we selected for the masks only the lines of the elements generating the strongest magnetic signal in the Stokes *V* spectra. Furthermore, only the best lines that appear to be unblended or minimally blended in the Stokes *I* spectra were included in the line mask.

Appendix B: Characteristic spectral lines in individual targets

In Figs. B.1–B.7 we show the integrated light (Stokes *I*) spectra of all sources studied in this Letter.

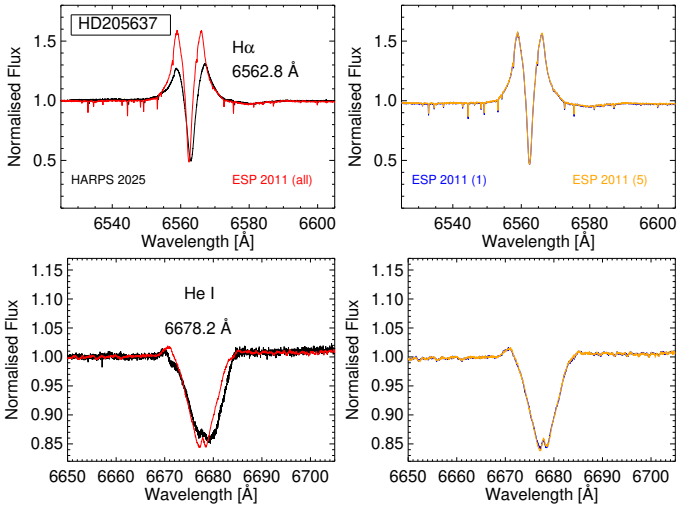

Fig. B.3. Emission in the Hα and the He I 6678 line profiles of HD 205637 observed in the ESPaDOnS and HARPSpol Stokes *I* spectra. *Top left:* All five ESPaDOnS Hα profiles overplotted with the one observed in the HARPSpol spectrum. *Top right*: Only the first and last ESPaDOnS Hα profiles are overplotted, showing no changes over 0.8 h. *Bottom:* Same but for the He I 6678 line profile.

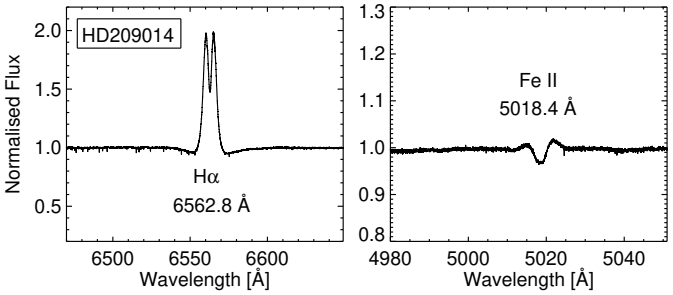

Fig. B.4. Emission in the Hα line and in both the red and blue wings of the profile of the Fe II 5018 line observed in the HARPSpol Stokes *I* spectrum of HD 209014.

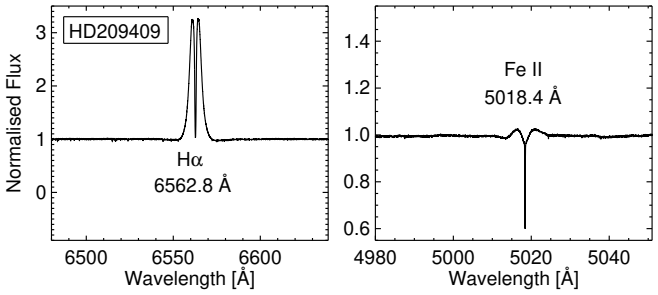

Fig. B.5. Strong emission in the Hα line and the sharp core in the profile of the Fe II 5018 line observed in the HARPSpol Stokes *I* spectrum of HD 209409.

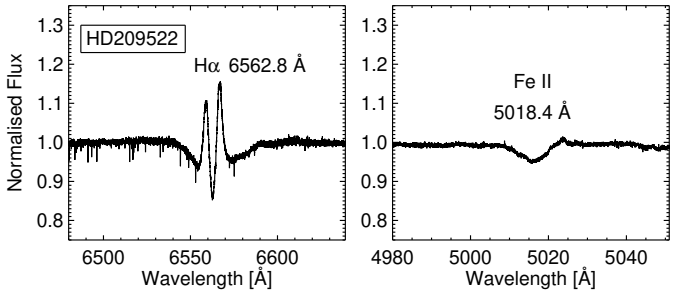

Fig. B.6. Hα emission in the HARPSpol Stokes I spectrum of the Be star HD 209522. We also observe a weak emission in the red wing of the Fe II line at 5018 Å.

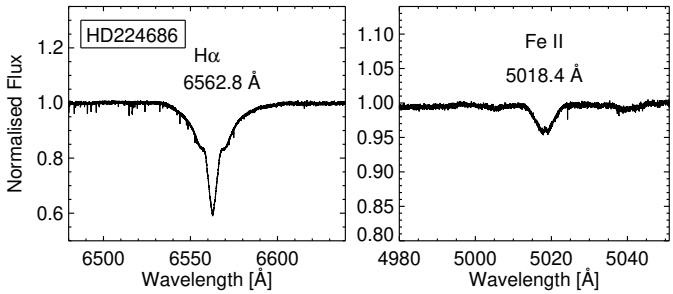

Fig. B.7. HARPSpol Stokes I spectrum of HD 224686 displaying the typical characteristic of a shell star, with the Hα line exhibiting a sharp absorption core. The profile of the Fe II 5018 line appears slightly split, most probably due to the presence of emission.